

Single-polarization single-mode hollow-core negative curvature fiber with nested U-type cladding elements

Qi-Wei Wang(王启伟), Shi Qiu(邱石), Jin-Hui Yuan(苑金辉), Gui-Yao Zhou(周桂耀), Chang-Ming Xia(夏长明), Yu-Wei Qu(屈玉玮), Xian Zhou(周娴), Bin-Bin Yan(颜玢玢), Qiang Wu(吴强), Kui-Ru Wang(王葵如), Xin-Zhu Sang(桑新柱), and Chong-Xiu Yu(余重秀)

Citation: Chin. Phys. B, 2022, 31 (**6**): 064213. DOI: 10.1088/1674-1056/ac46c7
Journal homepage: http://cpb.iphy.ac.cn; http://iopscience.iop.org/cpb

What follows is a list of articles you may be interested in

Single-mode antiresonant terahertz fiber based on mode coupling between core and cladding

Shuai Sun(孙帅), Wei Shi(史伟), Quan Sheng(盛泉), Shijie Fu(付士杰), Zhongbao Yan(闫忠宝), Shuai Zhang(张帅), Junxiang Zhang(张钧翔), Chaodu Shi(史朝督), Guizhong Zhang(张贵忠), and Jianquan Yao(姚建铨)

Chin. Phys. B, 2021, 30 (**12**): 124205. DOI: 10.1088/1674-1056/ac032e

A low-threshold multiwavelength Brillouin fiber laser with double-frequency spacing based on a small-core fiber

Lu-Lu Xu(徐路路), Ying-Ying Wang(王莹莹), Li Jiang(江丽), Pei-Long Yang(杨佩龙), Lei Zhang(张磊), and Shi-Xun Dai(戴世勋)

Chin. Phys. B, 2021, 30 (**8**): 084210. DOI: 10.1088/1674-1056/abff47

Visible-light all-fiber vortex lasers based on mode selective couplers

Chuchu Dong(董楚楚), Jinhai Zou(邹金海), Hongjian Wang(王鸿健), Han Yao(尧涵), Xianglong Zeng(曾祥龙), Yikun Bu(卜轶坤), Zhengqian Luo(罗正钱)

Chin. Phys. B, 2020, 29 (**9**): 094204. DOI: 10.1088/1674-1056/aba278

Polarization control and tuning efficiency of tunable vertical-cavity surface-emitting laser with internal-cavity sub-wavelength grating

Xiao-Long Wang(王小龙), Yong-Gang Zou(邹永刚), Zhi-Fang He(何志芳), Guo-Jun Liu(刘国军), Xiao-Hui Ma(马晓辉)

Chin. Phys. B, 2020, 29 (**8**): 084208. DOI: 10.1088/1674-1056/ab9442

Observation of wavelength-switchable solitons in an all-polarization-maintaining erbium-doped fiber cavity based on graphene saturable absorber reflector

Kuo Meng(孟阔), Lian-Qing Zhu(祝连庆), Fei Luo(骆飞)

Chin. Phys. B, 2017, 26 (**1**): 014205. DOI: 10.1088/1674-1056/26/1/014205

Single-polarization single-mode hollow-core negative curvature fiber with nested U-type cladding elements

Qi-Wei Wang(王启伟)[1], Shi Qiu(邱石)[1], Jin-Hui Yuan(苑金辉)[1,2,†], Gui-Yao Zhou(周桂耀)[3], Chang-Ming Xia(夏长明)[3], Yu-Wei Qu(屈玉玮)[1], Xian Zhou(周娴)[2], Bin-Bin Yan(颜玢玢)[1], Qiang Wu(吴强)[4,‡], Kui-Ru Wang(王葵如)[1], Xin-Zhu Sang(桑新柱)[1], and Chong-Xiu Yu(余重秀)[1]

[1] *State Key Laboratory of Information Photonics and Optical Communications, Beijing University of Posts and Telecommunications, Beijing* 100876, *China*
[2] *Research Center for Convergence Networks and Ubiquitous Services, University of Science & Technology Beijing, Beijing* 100083, *China*
[3] *Guangzhou Key Laboratory for Special Fiber Photonic Devices, South China Normal University, Guangzhou* 510006, *China*
[4] *Department of Physics and Electrical Engineering, Northumbria University, Newcastle upon Tyne, NE*1 8*ST, United Kingdom*

(Received 1 November 2021; revised manuscript received 22 December 2021; accepted manuscript online 29 December 2021)

Hollow-core negative curvature fibers (HC-NCFs) have become one of the research hotspots in the field of optical fiber because of their potential applications in the data and energy transmissions. In this work, a new kind of single-polarization single-mode HC-NCF with nested U-type cladding elements is proposed. To achieve the single-polarization single-mode transmission, we use two different silica tubes in thickness, which satisfy the resonance and anti-resonance conditions on the U-type cladding elements and the cladding tubes, respectively. Besides, the elliptical elements are introduced to achieve good single-mode performance. By studying the influences of the structure parameters on the propagation characteristics, the optimized structure parameters are obtained. The simulation results show that when the wavelength is fixed at 1550 nm, the single-polarization single-mode transmission is achieved, with the polarization extinction ratio of 25749 and minimum high-order mode extinction ratio of 174. Furthermore, the confinement loss is only 0.0015 dB/m.

Keywords: hollow-core negative curvature fiber, single-polarization, single-mode, finite element method

PACS: 42.81.Gs, 42.68.Ay, 42.25.Bs, 42.81.–i **DOI:** 10.1088/1674-1056/ac46c7

1. Introduction

Hollow-core negative curvature fiber (HC-NCF), whose surface is perpendicular to the boundary of the core, is opposite to the radial unit vector in the cylindrical coordinate system, and their transmission mechanism results from the anti-resonance reflection.[1–6] Unlike the hollow-core photonic bandgap fiber (HC-PBGF), there is no periodically arranged cladding structure in the HC-NCF.[7–11] In addition, the HC-NCF has a broader bandwidth and lower transmission loss because of its large core diameter and special transmission mechanism.[12–17] For an optical communication system, if the optical fiber has good single-polarization characteristic, it can avoid the effects of the polarization mode dispersion and crosstalk between the polarization modes during transmission.[18–20] In recent years, some investigators did their best to achieve the single-polarization characteristics of the NC-HCFs.[21–25] Now, there are the two main methods to design the single-polarization HC-NCFs. The first method is to introduce the symmetrical refractive index distributions. By filling or coating high refractive index materials in the cladding tubes in one direction, the coupling strength between the fundamental mode (FM) and silica modes (SMs) in the direction will be enhanced, which leads to a high confinement loss (CL).[26,27] The other method is to design a symmetrical geometric structure. By keeping the thickness of the silica tubes in one direction to meet the resonance condition, while the thickness of the silica tubes in the other direction meet the anti-resonance condition. At this time, the coupling strength between the FM and SM in one direction will be enhanced and restrained in the other direction.[21,22,28]

In 2015, Mousavi and Richardson reported a nested anti-resonance nodeless fiber (NANF) with four silica tubes, which is the first single-polarization anti-resonant fiber. The polarization extinction ratio (PER) is approximately 1000 and lowest-loss polarization is 0.075 dB/m.[21] In 2018, Wei *et al.* demonstrated the polarization-maintaining NCFs with six silica tubes. By introducing the resonant thickness on the nested tubes in the *y*-polarization direction, the PER is 850, and the lowest-loss polarization is 0.02 dB/m at wavelength 1550 nm.[23] In 2018, Yan *et al.*[24] proposed a double-ring HC-NCF with six tubes. By introducing resonant thickness on the inner tubes in the *x*-polarization direction, the PER is 17662, and the lowest-loss polarization is 0.04 dB/m at wavelength 1550 nm. Besides, this proposed HC-NCF has a good single-mode transmission performance with a high-order mode extinction ratio (HOMER) of 393.[24] In 2020, Yerolatsitis *et al.* fabricated a single-mode birefringent NCF with six silica tubes. By introducing different tubes in thickness in

†Corresponding author. E-mail: yuanjinhui81@bupt.edu.cn
‡Corresponding author. E-mail: qiang.wu@northumbria.ac.uk

© 2022 Chinese Physical Society and IOP Publishing Ltd

the x direction, the measured CL is 0.46 dB/m at wavelength 1550 nm with a birefringence of 2.5×10^{-5}.[25] From the previous researches, the high-order mode suppression and low loss characteristics can be significantly improved by introducing the elliptical silica tubes in the cladding region in comparison with the case of circular silica tubes.[29,30]

In this paper, we propose a single-polarization single-mode HC-NCF with nested U-type cladding elements. The influences of the structure parameters on the PER and CL are investigated by the finite element method (FEM). In this design, to guarantee the low CL, we first introduce the eight elliptical cladding silica tubes, whose thickness meet satisfy the anti-resonance condition. Second, in order to achieve the single-polarization characteristic, we add the two U-type silica elements in the y-polarization direction, whose thickness meet the resonance condition. Thus, it satisfies not only the asymmetry of the tube thickness in the two transverse orthogonal directions, but also the asymmetry of the tube shape. The simulation results show that the proposed HC-NCF can achieve single-polarization single-mode guidance with a PER of 25749 and an HOMER of 174. Moreover, the x-polarization fundamental mode loss of the HC-NCF is only 0.0015 dB/m, and the HC-NCF shows a good bending-resistance.

2. Design of single-polarization single-mode HC-NCF and performances

The cross-section of the proposed HC-NCF is shown in Fig. 1. Compared with the traditional nested tube HC-NCFs, such a U-type nested tube structure can avoid the high refractive index points caused by the connection between the outer tube and nested tube. Therefore, the lower CL for the HC-NCF can be achieved. As shown in Fig. 1, the major axial radius and minor axis radius for each of the two elliptical tubes in the y direction are r_1 and r_2, respectively. The arc part of the nested U-type silica tube is a semicircle, whose radius is r_5, and the distance between the bottom of the U-typed silica tube and the top of the outer silica tube is $2r_5$. The other six elliptical cladding silica tubes have the same major axis radius r_3 and minor axis radius r_4. There are two kinds of tubes. The thickness for each of the two U-type nested silica tubes (green color) is t_2, and the thickness of the remaining tubes is t_1. The inner core radius and outer core radius are denoted as R_1 and R_2. And the relationship between R_2 and other parameters can be described as

$$R_2 = R_1 + 2r_3 - 2r_1. \tag{1}$$

The transmission mechanism of the HC-NCFs results from the anti-resonant reflecting optical waveguide (ARROW) mode.[11] When the fiber structure satisfies the resonance condition, the thickness of the silica tubes can be obtained from

$$t = m\lambda/[2(n_{\text{glass}}^2 - n_{\text{air}}^2)^{1/2}]. \tag{2}$$

When the fiber structure satisfies the anti-resonance condition, the corresponding thickness of the silica tubes can be expressed as

$$t = (m-0.5)\lambda/[2(n_{\text{glass}}^2 - n_{\text{air}}^2)^{1/2}], \tag{3}$$

where the positive integer m is the resonance order, λ (in unit nm) is the operating wavelength, n_{glass} is the refractive index of the silica, and n_{air} is the refractive index of the air.

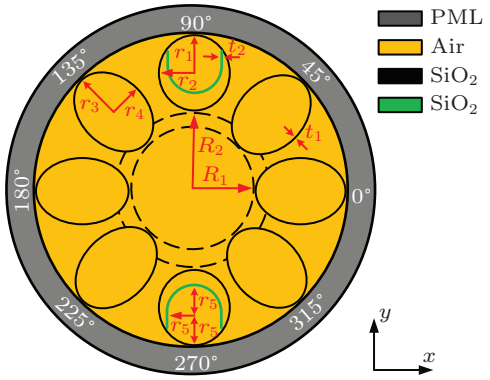


Fig. 1. Cross-section structure of designed single-polarization single-mode HC-NCF with nested U-type cladding elements.

When the FM is coupled with the SM, the CL of the FM will increase. The CL can be obtained from[3]

$$\text{CL(dB/m)} = 40\pi n_{\text{imag}}/[\ln(10)\lambda], \tag{4}$$

where n_{imag} is the imaginary part of the effective refractive index of the guided mode.

The PER is defined as the loss ratio of the y-polarization FM to the x-polarization FM, and expressed as

$$\text{PER} = \text{loss}_{y-\text{pol}}/\text{loss}_{x-\text{pol}}, \tag{5}$$

where the loss of the FM is defined as the ratio of the minimum value of the loss of FM in y polarization to the minimum value of the loss of FM in x polarization. In this work, when the PER is higher than 100 or lower than 0.01, it can be regarded as the single-polarization guidance.

The bending loss is a very important parameter in the practical application. We use the conformal transformation method to make the refractive index in the optical fiber equivalent to[21]

$$n'(x,y) = n(x,y)(1 + x/R_{\text{bend}}), \tag{6}$$

where $n'(x,y)$ is the equivalent refractive index, $n(x,y)$ is the original refractive index, and R_{bend} is the bending radius. Here, we assume that the bending direction is along the x axis.

In this work, the low loss and single-polarization characteristics of the proposed HC-NCF can be achieved by adjusting the structure parameters. For the outer rings of the two

silica tubes in the y direction, the tube thickness is set to be the anti-resonant thickness to ensure the low CL of the FM. To introduce the single-polarization characteristic, the thickness values of the two nested U-type tubes in the y direction satisfy the resonance condition. According to Eqs. (2) and (3), for $m = 2$, $t_1 = 1.12$ μm is an anti-resonant thickness at wavelength 1550 nm, and $t_2 = 1.5$ μm is a resonant thickness at wavelength 1550 nm. Thus, the initial structure parameters of the HC-NCF are set to be $R_1 = 16$ μm, $r_1 = 15$ μm, $r_2 = 13$ μm, $r_3 = 19$ μm, $r_4 = 15$ μm, $r_5 = 15$ μm, $t_1 = 1.12$ μm, and $t_2 = 1.5$ μm. The FEM is adopted to simulate the proposed HC-NCF. In this simulation, the perfectly matched layer (PML) is added to the outermost layer, the grid size of the air area is set to be $\lambda/3$, and other silica regions are assumed to be $\lambda/6$.

Figures 2(a) and 2(b) show the calculated mode field distributions of the y-polarization silica mode (SM_1) at wavelength 1540 nm and x-polarization silica mode (SM_2) at wavelength 1554 nm, respectively. Figures 2(c) and 2(d) show the mode field distributions of the y-polarization fundamental mode (FM_1) at wavelength 1552 nm and x-polarization fundamental mode (FM_2) at wavelength 1556 nm, respectively.

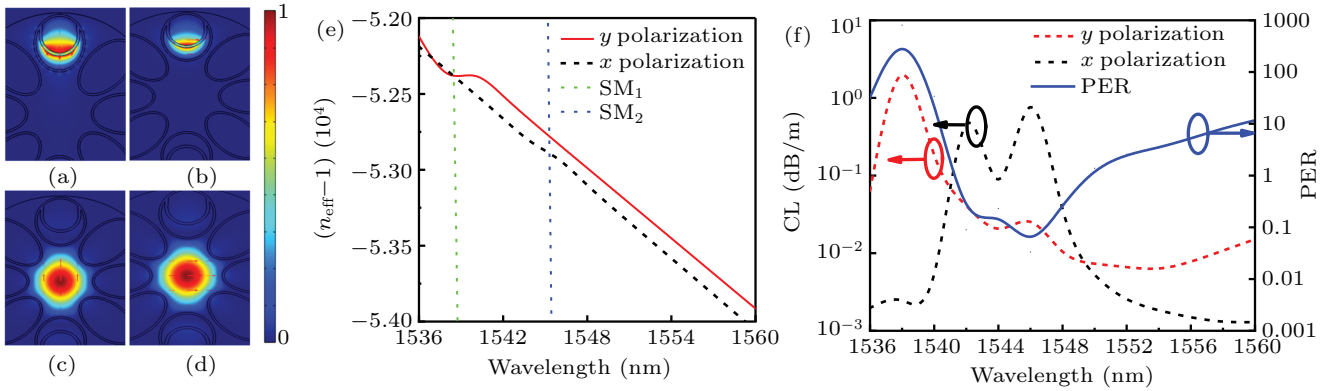


Fig. 2. (a)–(d) Mode field distributions of SM_1 at wavelength 1540 nm, SM_2 at wavelength 1554 nm, FM_1 at wavelength 1552 nm, and FM_2 at wavelength 1556 nm. (e) Effective refractive index curves of x-polarization and y-polarization FMs and two SMs. (f) CL curves of x-polarization FM and y-polarization FM, and the corresponding PER.

Figure 2(e) shows that the SM_1 is coupled with the FM_1 at wavelength 1538 nm, whereas the SM_2 is coupled with the FM_2 at wavelength 1546 nm. Figure 2(e) shows the plots of the real part of the effective refractive index of the x-polarization FM, y-polarization FM and two SMs *versus* wavelength. At wavelength 1538 nm, the effective refractive index curves of the FM_1 and SM_1 intersect, and the FM_1 is coupled with the SM_1 at this time. At wavelength 1546 nm, the effective refractive index curves of the FM_2 and SM_2 intersect, and the FM_2 is coupled with the SM_2 at this time. Figure 2(f) shows the CL curves of the x-polarization and y-polarization FMs and their corresponding PER. As seen from Fig. 2(e), when the FM_1 is coupled with the SM_1 at wavelength 1538 nm, the CL of the FM_1 increases, but the CL of the FM_2 changes slightly. When the FM_2 is coupled with the SM_2 at wavelength 1546 nm, the CL of the FM_2 increases, while the CL of the FM_1 changes slightly. When $\lambda = 1550$ nm, the PER is 102, and the CL is 0.017 dB/m. In the following, we will discuss how to improve the PER and reduce the CL around 1550 nm.

3. Influences of fiber structure parameters on propagation characteristics

To obtain the higher PER and lower CL, the influences of the fiber structure parameters need discussing. From the analysis in Section 2, it is known that t_1 has the greatest influence on the CL and t_2 has the greatest influence on the PER. Thus, we first fix t_1 at a determined value and study the influence of t_2 on the PER. Figure 3(a) shows the plots of PER calculated *versus* t_2, with t_1 fixed separately at 1.116, 1.118, and 1.12 μm. It can be seen from Fig. 3(a) that with the increase of t_2, the PER peak wavelengths are shifted, but the PER peak can be obtained by adjusting the value of t_1 and t_2 reasonably. Therefore, a pair of t_1 and t_2 can be chosen to obtain a better single-polarization characteristic. We choose $t_1 = 1.116$ μm and $t_2 = 1.51$ μm to obtain the highest PER according to Fig. 3(a). Figure 3(b) shows the CL of the x-polarization and y-polarization FMs and corresponding PER when t_1 is fixed at 1.116 μm at wavelength 1550 nm. It is found that when $t_2 = 1.51$ μm, the CL of the x-polarization FM is the lowest and the CL of the y-polarization FM is the highest . As t_2 changes, the CL of the x-polarization FM experiences a small change, but the CL of the y-polarization FM has a great change. The main reason is that when t_2 changes, the coupling wavelength and coupling degree of the y-polarization FM and SM_1 will change, which will result in the change of the wavelength corresponding to the high loss point in the y-polarization direction and PER.

Figure 4(a) shows that the PER and CL of the proposed HC-NCF vary with wavelength in a range from 1545 nm to

1555 nm for three different values of t_1. When t_1 increases from 1.116 μm to 1.12 μm, a red-shift happens to the PER peak wavelength, and the PER peak value decreases. The reason is that with the increase of t_1, the coupling wavelengths of the y-polarization FM and SM_1 will trigger off a red-shift, and the coupling degree will decrease. However, the CL has little change when t_1 changes. Figure 4(b) shows that the PER and CL vary with wavelength in a range from 1545 nm to 1555 nm for three different values of t_2. When t_2 increases from 1.51 μm to 1.514 μm, a red-shift happens to the PER peak wavelength , and the PER peak value increases. The reason is that with the increase of t_2, the coupling wavelength of the y-polarization FM and SM_1 will set up the red-shifts and the coupling degrees will increase. However, when t_2 changes, the CL has little change.

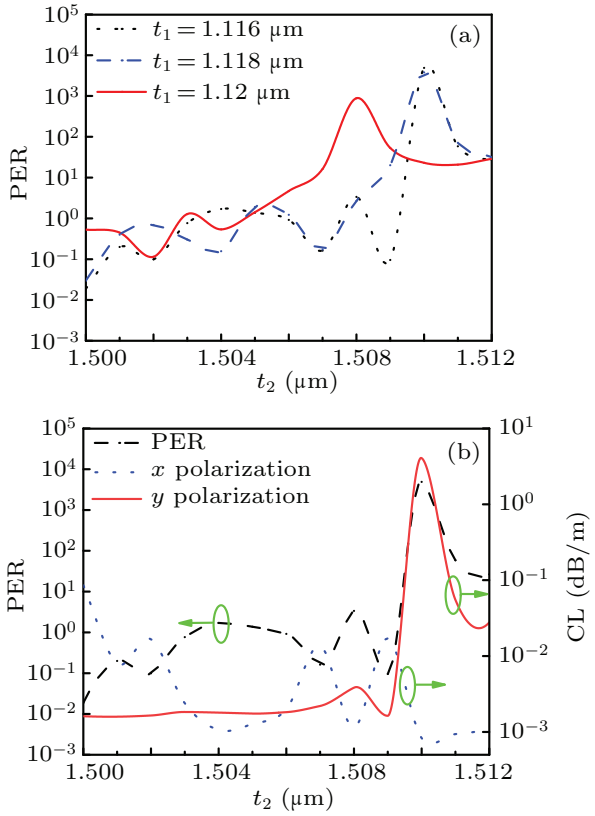


Fig. 3. (a) Plots of PER *versus* t_2, with t_1 fixed separately at 1.116, 1.118, and 1.12 μm at wavelength 1550 nm. (b) Plots of CL of the x-polarization and y-polarization FMs and corresponding PER *versus* t_2, with t_1 fixed at 1.116 μm at wavelength 1550 nm.

Figures 5(a)–5(f) show the calculated PERs and CLs of the proposed HC-NCF when r_1, r_2, r_3, r_4, r_5, and R_1 are changed, respectively. From Fig. 5(a), when r_1 increases from 14.5 μm to 15.5 μm, these PER peak wavelengths give rise to red-shifts, and are located at 1549, 1551, and 1552 nm, respectively, corresponding to the PER values of 1561, 16772, and 1310. From Fig. 5(b), when r_2 increases from 12.5 μm to 13.5 μm, the PER peak wavelengths cause red-shifts, and are located at 1549, 1551, and 1552 nm, respectively, with the PER values being 526, 16772, and 533. Figure 5(c) shows that when r_3 increases from 17.5 μm to 18.5 μm, the PER peak wavelengths present red-shifts, and are located at 1550, 1551, and 1551 nm, respectively, with the PER values being 5267, 16772, and 21287. Figure 5(d) indicates that when r_4 increases from 18.5 to 19.5 μm, the PER peak wavelengths have small shifts and are located at 1551 nm, with the PER values being 11287, 16772, and 29735. From Fig. 5(e) it follows that when r_5 increases from 14.5 μm to 15.5 μm, the PER peak wavelengths have blue shifts, and are located at 1552, 1551, and 1548 nm, respectively, with the PER values being 317, 16772, and 497. From Fig. 5(f) it follows that when R_1 increases from 15.5 μm to 16.5 μm, the PER peak wavelengths set up red-shifts, and are located around 1551 nm, with the PER values being 5036, 16772, and 27007. The main reason can be that as r_1, r_2, r_3, r_4, r_5 or R_1 change, the coupling wavelength and coupling degree of the y-polarization FM and SM_1 will change, which will result in the change of the wavelength corresponding to the high loss point in the y-polarization direction and PER. However, from Figs. 5(a)–5(f), the CL has little change whenr_1, r_2, r_3, r_4, r_5 or R_1 change. In summary, it can be concluded that when t_1 and t_2 are fixed, the other structure parameters of the proposed HC-NCF have different effects on the PER.

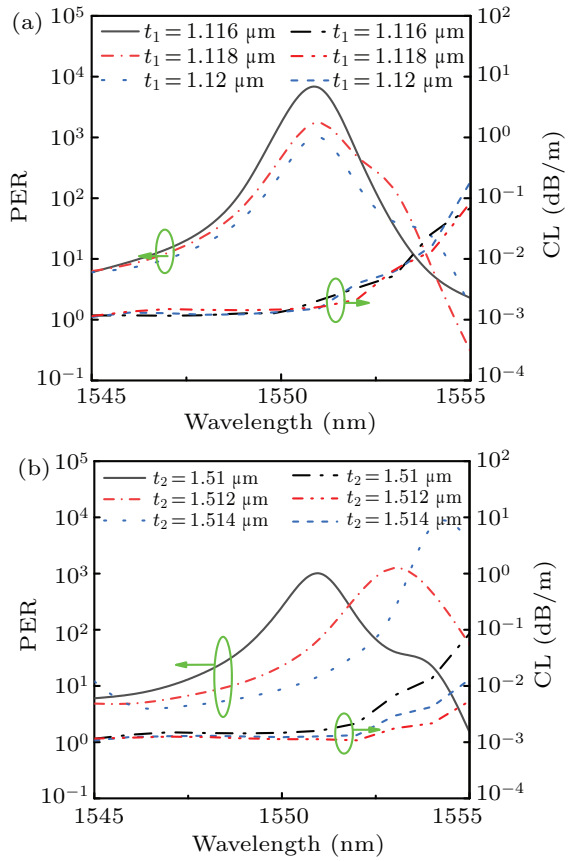


Fig. 4. Curves of PER and CL, (a) with t_1 being 1.116, 1.118, and 1.12 μm. and t_2 being 1.51 μm, and (b) with t_2 being 1.51, 1.512, and 1.514 μm and t_1 being1.116 μm separately.

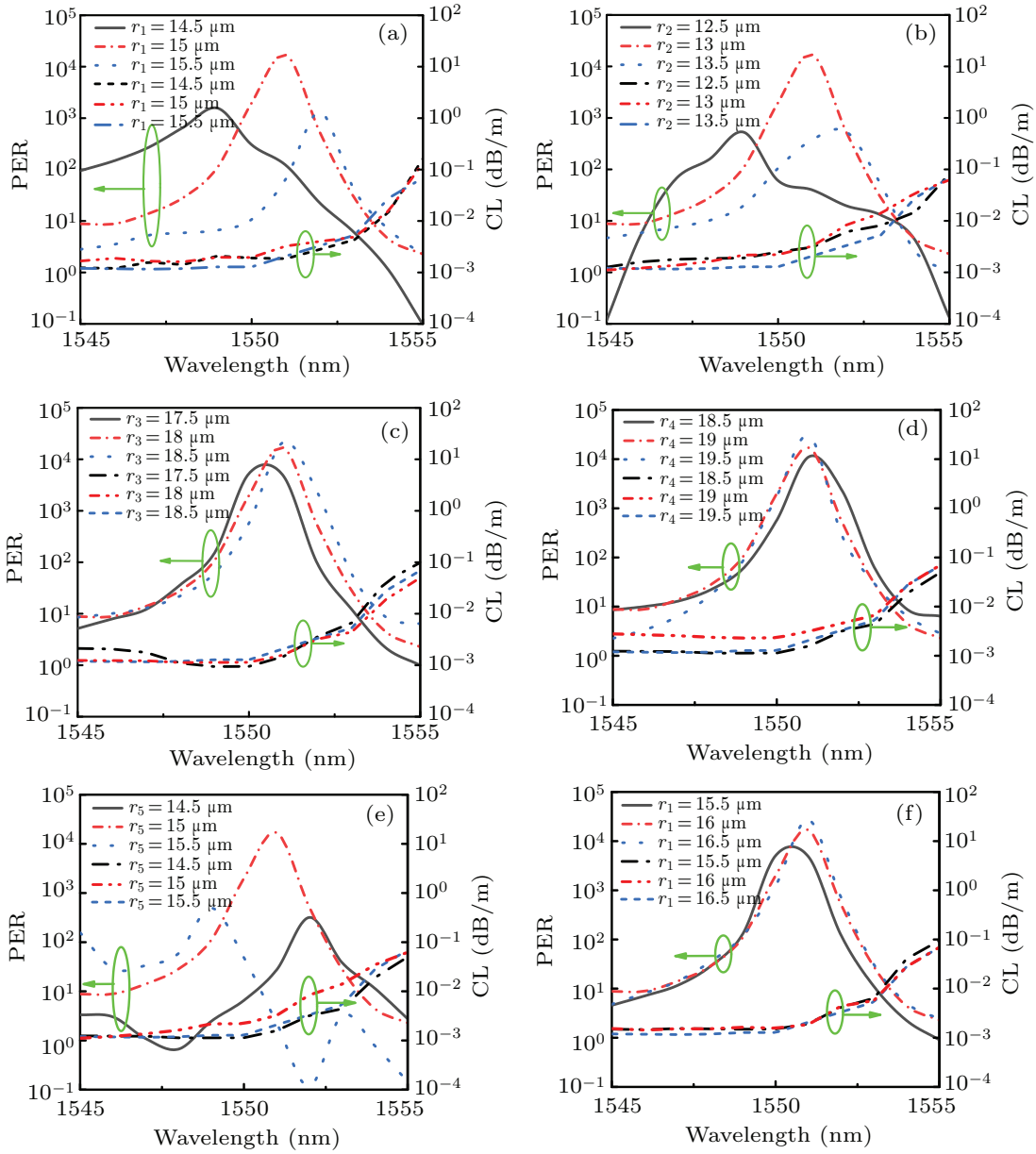


Fig. 5. Curves of PER and CL (a), with r_1 being 14.5, 15, and 15.5 μm; (b) with r_2 being 12.5, 13, and 13.5 μm; (c) with r_3 being 17.5, 18, and 18.5 μm; (d) with r_4 being 18.5, 19, and 19.5 μm; (e) with r_5 being 14.5, 15, and 15.5 μm; and (f) with R_1 being 15.5, 16, and 16.5 μm, separately.

4. Transmission performances of proposed HC-NCF

Based on the above analyses, the final structural parameters of the HC-NCF are determined as follows: $R_1 = 16$ μm, $r_1 = 15$ μm, $r_2 = 13.2$ μm, $r_3 = 19$ μm, $r_4 = 15.3$ μm, $r_5 = 15$ μm, $t_1 = 1.115$ μm, and $t_2 = 1.507$ μm. Figure 6(a) shows the variations of real parts of the effective refractive indices of the *x*-polarization and *y*-polarization FMs and two SMs with wavelength. It can be seen from Fig. 6(a) that at wavelengths 1522, 1529, and 1550 nm, the effective refractive index curves of the *y*-polarization FM and SM_1 intersect, and the effective refractive index curve of the *y*-polarization FM has a sudden change. At 1556 nm, the effective refractive index curves of the *x*-polarization FM and SM_2 intersect, and the effective index curve of the *x*-polarization FM has a sudden change. In Fig. 6(c), at wavelengths 1522 nm, 1529 nm, and 1550 nm, the effective refractive index curve of the *y*-polarization FM has a sudden change, and the CL of the *y*-polarization FM will increase sharply. In contrast, the CL of the *x*-polarization FM changes slightly. And at 1556 nm, when the effective refractive index curve of the *x*-polarization FM has a sudden change, the CL of the *x*-polarization FM will increase sharply, but the CL of the *y*-polarization FM changes slightly. In Fig. 6(d), there will be extreme values of the PER respectively near the wavelengths 1522 nm, 1529 nm, 1550 nm, and 1556 nm, and there exist two single-polarization regions in the wavelength range from 1521 nm to 1522 nm and from 1548 nm to 1551 nm.

Besides, at 1550 nm, the PER is 25749, and the CL of the FM is 0.00152 dB/m.

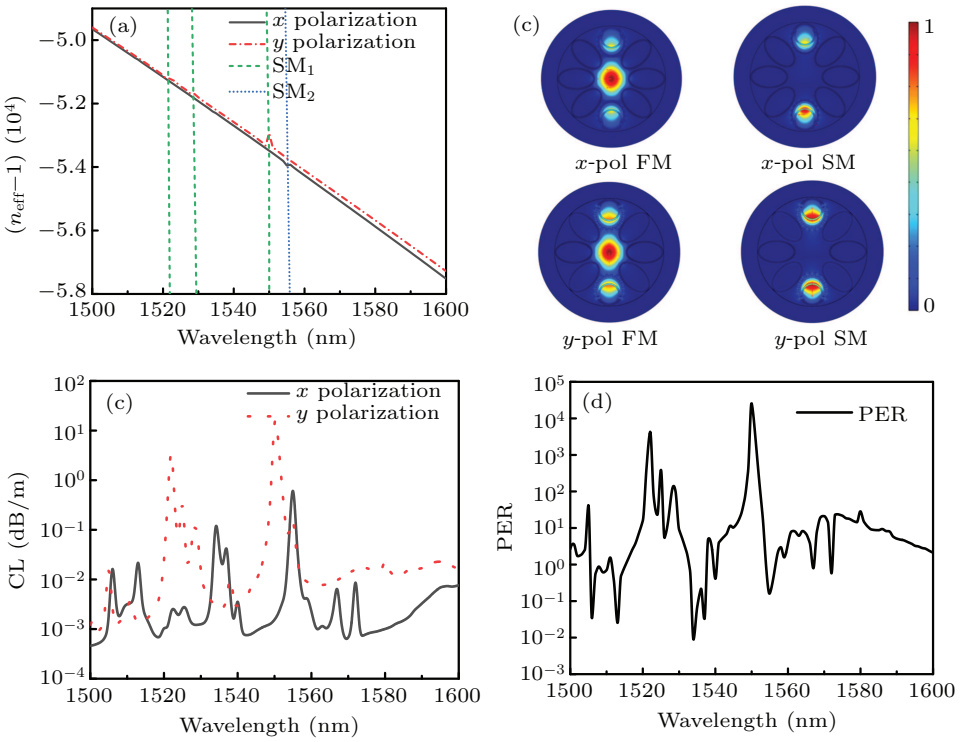


Fig. 6. (a) Wavelength-dependent effective refractive indices of *x*-polarization (*x*-pol) and *y*-polarization (*y*-pol) FMs and two SMs; (b) electric field distributions of *x*-polarization FM, *x*-polarization SM at wavelength 1556 nm and *y*-polarization FM, *y*-polarization SM at wavelength 1550 nm; (c) wavelength-dependent loss of *x*-polarization and *y*-polarization FMs; and (d) wavelength-dependent PER.

In this work, the HOMER is defined as the minimum loss ratio of the loss of the higher-order modes to the fundamental loss. At 1550 nm, the HOMER is 174, so the proposed HC-NCF can be regarded as the single-mode guidance.

5. Bending loss characteristic of proposed HC-NCF

Figure 7(a) shows the bending loss of the FM_1 and the FM_2, which are represented, respectively, by the red curve and the dark curve at wavelength 1550 nm. The extreme for $R_{\text{bending}} = 5$ cm is caused by the phase-matching between the core mode and cladding mode after bending for the two fundamental modes. Figures 7(b)–7(d) show the mode field distribution of the *x*-polarization FM calculated with $R_{\text{bending}} = 2$, 5, and 8 cm. It can be found from Figs. 7(b)–7(d) that when the HC-NCF is bent along the *x* polarization with different values of R_{bending}, the mode field energy can be well confined in the core region of the HC-NCF.

Table 1 shows the comparison between the results of the PER, CL, and HOMER of the proposed HC-NCF and the results of other researches. It can be seen from Table 1 that the proposed HC-NCF has the highest PER and the lowest CL. Thus, it has good single-polarization single-mode transmission characteristic.

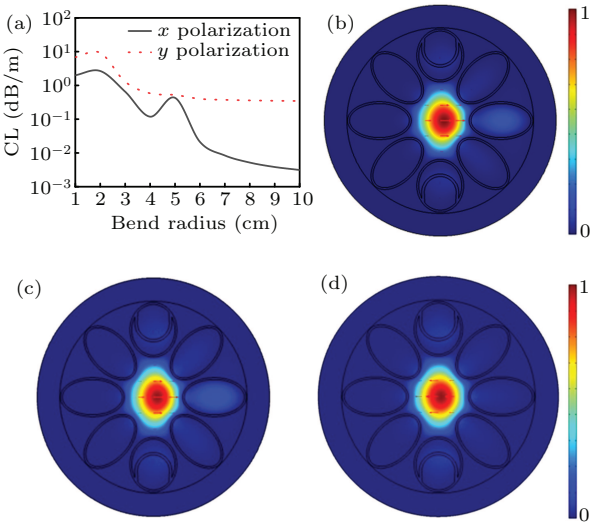


Fig. 7. (a) Curves of calculated bending loss at wavelength 1550 nm, and (b) mode-field distribution of *x*-polarization FM separately with $R_{\text{bending}} =$ 2 cm, (c) 5 cm, and (d) 8 cm.

Table 1. Comparison of results between proposed HC-NCF and other researches.

Ref.	Structures	PER	CL (dB/m)	HOMER
[26]	four-tube HC-NCF	1000	0.04	N/A
[28]	hollow core nested ant-resonant nodeless fibers (HC-NANF)	850	0.02	N/A
[21]	double-ring HC-NCF	17662	0.04	393
[22]	six-tube HC-NCF	N/A	0.46	N/A
This work	U-type cladding elements HC-NCF	25749	0.0015	174

6. Conclusions

In this work, we proposed a novel single-polarization single-mode HC-NCF that includes two nested U-typed silica tubes. When the fundamental mode and the nested U-typed silica tube mode in the same polarization direction are coupled with each other, the CL of the fundamental mode in the polarization direction will increase, and the PER will increase at the same time. The simulation results show that for the proposed HC-NCF, the CL is only 0.0015 dB/m, the PER can reach 25749, and the HOMER is 174. The proposed HC-NCF has a good single-polarization single-mode transmission characteristic. It is believed that such an HC-NCF will be very useful in transferring the data and energy.

Acknowledgement

Project supported by the National Natural Science Foundation of China (Grant No. 61935007).

References

[1] Vincetti L and Setti V 2010 *Opt. Express* **18** 23133
[2] Pryamikov A D and Biriukov A S and Kosolapov A F and Plotnichenko and Semjonov S L and Dianov E 2011 *Opt. Express* **19** 1441
[3] Wei C, Weiblen R J and Menyuk C R and Hu J 2017 *Adv. Opt. Photon.* **9** 504
[4] Zhao X T and Xiong Q and Jiang G H and Cheng J R and Wang S T 2018 *Opt. Fiber Technol.* **46** 167
[5] Kolyadin A N and Alagashev G K and Pryamikov A D and Mouradian L and Zeytunyan A and Toneyan H and Kosolapov A F and Bufetov I A 2015 *Phys. Rep.* **73** 59
[6] Belardi W and Knight J C J O L 2014 *Opt. Lett.* **39** 1853
[7] Liu M and Hou J Y and Yang X and Zhao B Y and Shum P 2018 *Chin. Phys. B* **27** 014206
[8] Haakestad M W, Causality J S and Kramers-Kronig 2005 *Opt. Express* **13** 9922
[9] Argyros A and Pla J 2007 *Opt. Express* **15** 7713
[10] Broeng J, Barkou S E, Søndergaard T and Bjarklev A 2000 *Opt. Lett.* **25** 96
[11] Zhang Y S, Yuan J H, Qu Y W, Zhou X, Yan B B, Wu Q, Wang K R, Sang X Z, Long K P and Yu C X 2020 *Chin. Phys. B* **29** 034208
[12] Yu F, Wadsworth W J and Knight J C 2012 *Opt. Express* **20** 11153
[13] Hasan M I, Akhmediev N and Chang W 2017 *Opt. Lett.* **42** 703
[14] Yu T Y, Liu X and Fan Z W 2017 *IEEE Photon. J.* **10** 1
[15] Nawazuddin M B S, Wheeler N V, Hayes J R, Sandoghchi S R, Bradley T D, Jasion G T, Slavík R, Richardson D J and Poletti F 2017 *J. Lightw. Technol.* **36** 1213
[16] Provino L J F 2018 *Fibers* **6** 42
[17] Qiu S, Yuan J H, Zhou X, Li F, Wang Q W, Qu Y W, Yan B B, Wu Q, Wang K R, Sang X Z, Long K P and Yu C X 2020 *Sensors* **20** 6539
[18] Fu B, Li S G, Yao Y Y, Zhang L and Zhang M Y 2011 *Chin. Phys. B* **20** 024209
[19] Goel C and Yoo S 2020 *CLEO: Applications and Technology, Optical Society of America*, May 10–15, 2020, Washington DC, USA, pp. JW2E. 2
[20] Ankan I M, Mollah M A, Paul A K and Chakrabarti K 2020 *IEEE Region 10 Symposium*, June 5–7, 2020, Dhaka, Bangladesh, p. 612
[21] Yan S B, Lou S Q, Lian Z G, Zhang W and Wang X 2019 *J. Lightw. Technol.* **37** 5707
[22] Yan S B, Lian Z G, Lou S Q, Wang X, Zhang W and Tang Z J 2020 *IEEE Access* **8** 53419
[23] Ding W and Wang Y Y 2015 *Opt. Express* **23** 21165
[24] Mousavi S A, Richardson D J, Sandoghchi S R and Poletti F 2015 *European Conference on Optical Communication* September 27–October 1, 2015, Valencia, Spain, p. 1
[25] Fini J M, Nicholson J W, Mangan B, Meng L, Windeler R S, Monberg E M, DeSantolo A, DiMarcello F V and Mukasa K 2014 *Nat. Commun.* **5** 1
[26] Wei C L, Menyuk C R and Hu J 2018 *Opt. Express* **26** 9528
[27] Yan S B, Lou S Q, Zhang W and Lian Z G 2018 *Opt. Express* **26** 31160
[28] Yerolatsitis S, Shurvinton R, Song P, Zhang Y P, Francis-Jones R J A and Rusimova K R 2020 *J. Lightw. Technol.* **38** 5157
[29] Habib M S, Bang O and Bache M 2016 *Opt. Express* **24** 8429
[30] Meng F C, Liu B W, Li Y F, Wang C F and Hu M L 2016 *IEEE Photon. J.* **9** 1